INVESTIGATING THE LIGNOCELLULOSIC COMPOSITION DURING DELIGNIFICATION USING CONFOCAL RAMAN SPECTROSCOPY, CROSS-POLARIZATION MAGIC ANGLE SPINNING CARBON 13 - NUCLEAR MAGNETIC RESONANCE (CP/MAS ^{13}C-NMR) SPECTROSCOPY AND ATOMIC FORCE MICROSCOPY

V. CHUNILALL, T. BUSH and R. M. ERASMUS[*]

Forestry and Forest Products Research Centre, Natural Resources and Environment, CSIR, Congella, 4013, Durban, South Africa
[*]*Raman and Luminescence Laboratory, School of Physics, University of the Witwatersrand, Private Bag 3, WITS 2050, South Africa*

Changes in the lignocellulosic composition of four hardwoods, *i.e. Eucalyptus grandis camaldulensis (E. gc)*, *E. grandis urophylla (E. gu)*, *E. dunnii* and *E. nitens*, were investigated during different delignification processes using confocal Raman spectroscopy, Cross-Polarization Magic Angle Spinning Carbon 13 - Nuclear Magnetic Resonance (CP/MAS ^{13}C-NMR) spectroscopy and Atomic Force Microscopy (AFM) in conjunction with image analysis. The confocal Raman results evidenced differences in the distribution of lignin between the middle lamella and the secondary cell wall layer for all clones and species investigated. The *E. gc* clone showed high levels of lignin in the secondary cell wall layer, compared to the *E. gu* clone, *E. dunnii* and *E. nitens* species. CP/MAS ^{13}C-NMR spectroscopic results revealed an increase in cellulose crystallinity during chlorite delignification, acid bisulphite pulping and subsequent oxygen delignification, accompanied by an increase in the cellulose 'aggregate' area with a corresponding decrease in the 'matrix' area for each clone and species.

Keywords: atomic force microscopy, cellulose 'aggregate' area, cellulose crystallinity, confocal Raman spectroscopy, 'matrix' area, CP/MAS ^{13}C-NMR spectroscopy

INTRODUCTION

The structure of lignocellulosics in the wood cell wall occurs as a complex microstructure composed of lignin, extractives and hemicelluloses supporting bundles of tightly packed cellulose fibrils.[1] Cellulose, the major component of the cell wall, is a polysaccharide made up of (1-4)-β-D-glucopyranose units. After cellulose, hemicelluloses constitute the most abundant group of carbohydrates in the wood cell walls. Hemicelluloses are branched polymers made up of several monosaccharides. Lignin, the second most abundant polymer in wood, consists of phenyl propane units and plays an important supporting role. Hemicelluloses and lignin provide the 'matrix' in which cellulose fibrils are extensively cross-linked.[2] The wood cell wall is organised in several layers (Fig. 1). The wood cell wall consists of the middle lamella (ML), primary layer (P), secondary layers (S1, S2 and S3). Within the secondary cell wall layers, the S1, S2 and S3 differ with respect to the orientation of cellulose fibrils. The middle lamella surrounds the primary and secondary layers and holds the neighbouring wood cells together. Glucose is produced through photosynthesis. Haworth[4] proposed that the glucose units polymerise with the adjacent glucose units to form a long glucan chain. In this process, water is removed from the glucose and each individual unit is an anhydroglucose unit ($C_6H_{10}O_5$). Anhydroglucose units link up to form glucan chains. The linear glucan chains are linked laterally by hydrogen bonds to form linear aggregates,[5] thus giving rise to crystalline cellulose. Cellulose crystallinity

influences directly the accessibility of chemicals to chemical derivatisation, swelling and water-binding properties. Tensile strength, dimensional

stability and density increase with increasing crystallinity, while properties, such as chemical reactivity and cellulose swelling, decrease.
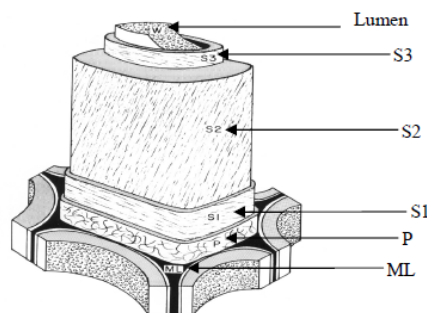

Figure 1: Simplified structure of the wood cell wall showing the middle lamella (ML), primary wall (P), secondary wall (S1, S2, S3) and lumen (L)[3]

The degree of crystallinity is a very important property and needs to be taken into account when considering the manufacturing and further applications of cellulose and cellulosic materials.[6] Cellulose crystallinity varies significantly, depending on the source of cellulose (hardwoods or softwoods), and type of pulping and bleaching processes applied. Cellulose crystallinity, which may be defined as the intensity fraction of the crystalline domains in lignocellulosic materials, has important effects on the physical, mechanical and chemical properties of cellulose.[7] A number of methods are available for the determination of cellulose crystallinity, including wide-angle X-ray scattering (WAXS),[8-10] Cross-Polarization Magic Angle Spinning Carbon 13-Nuclear Magnetic Resonance (CP/MAS ^{13}C-NMR) spectroscopy[11-13] and Fourier Transform - infrared (FT-IR) spectroscopy.[14] In this study, CP/MAS ^{13}C-NMR spectroscopy was used to determine the crystallinity of wood, holocellulose, unbleached acid bisulphite 'raw' and oxygen delignified pulp, washed 'D1' pulp samples from the clones (*i.e. E. gu, E. gc*) and species (*E. nitens, E. dunnii*).

Numerous techniques are currently available to quantitatively determine the amount of lignin in wood and pulp fibres. However, very few show the distribution of lignin within the cell walls (*i.e.* middle lamella and secondary cell wall layers). To provide a better understanding of the delignification process during chlorite delignification, acid bisulphite pulping and oxygen delignification, the distribution of lignin in the wood cell wall regions of the clones (*i.e. E. gu, E. gc*) and species (*E. nitens, E. dunnii*) was investigated using confocal Raman spectroscopy.

The Raman line scans for the wood samples were analysed in terms of the middle lamella (ML), secondary layer (S) and lumen regions. Changes in lignin intensity were recorded across the cell wall by tracking the Raman band for lignin centred at 1600 cm^{-1}. The location of cellulose and lignin-hemicelluloses-extractives 'matrix' area within the secondary cell wall layer can be also visualised by Atomic Force Microscopy (AFM) images. The 'aggregate' area in the secondary cell wall layer is assumed to be occupied by cellulose, whilst the 'matrix' areas are assumed to be occupied by lignin-hemicelluloses-extractives in wood and lignin-hemicelluloses in pulp.

EXPERIMENTAL

Materials

Four hardwoods, *i.e. Eucalyptus grandis camaldulensis (E. gc), Eucalyptus grandis urophylla (E. gu), E. dunnii* and *E. nitens,* were selected for the study and subjected to four different delignification processes, *i.e.* chlorite delignification for 4 and 9 h, acid bisulphite pulping, acid bisulphite pulping followed by oxygen delignification and 'D1' stage washing (Fig. 2).

Holocellulose delignification

Five grams of sawdust were added to a solution mixture containing 175 mL acetone and 75 mL water and left overnight (12 h) at room temperature, with stirring. After 12 h, the sawdust was washed three times with 250 mL deionised water. The chlorite solution was prepared by dissolving 2.5 g sodium chlorite ($NaClO_2$) in 75 mL deionised water, whilst adding 0.5 mL of glacial acetic acid to bring the pH in the range of 4-5. Thereafter, 5 g of the extracted sawdust were added to the 75 mL chlorite solution at

70 °C, with stirring for 4 and 9 h. The sawdust was then filtered and washed three times with 250 mL
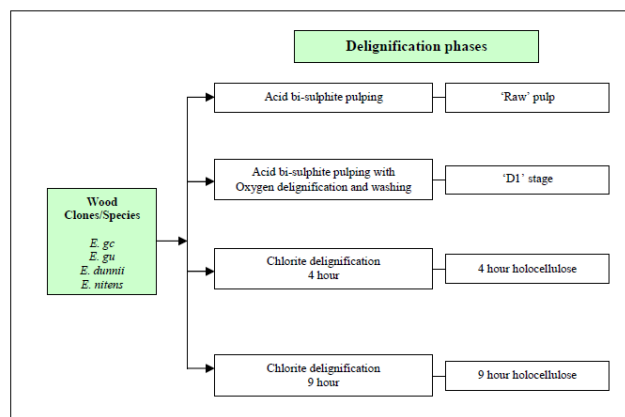
deionised water.

Figure 2: Flow diagram of delignification and bleaching processes applied to different clones and species

Acid bisulphite pulping

The pulping liquor was prepared by bubbling sulphur dioxide (SO_2) gas into a mixture of 70 g magnesium oxide (MgO) in 7 L of water and its circulation in a flow through digester containing 1700 g wood chips. Temperature was ramped to 140 °C and maintained for 90 min.

Oxygen delignification

Eight hundred grams of oven-dried acid bisulphite pulp was subjected to oxygen delignification at 400 kPa in a rotating digester. Pulp consistency was of 11%, with a caustic charge of 4% at a temperature of 100 °C for 80 min. After oxygen delignification, the pulp was treated with 1.4% chlorine dioxide at ca. 60 °C for 50 min.

Confocal Raman spectroscopy

The Raman spectra were acquired with a HORIBA Jobin-Yvon T64000™ confocal Raman Microscope with 514.5 nm excitation wavelength and a microscope attachment operating in single spectrograph mode with a grating of 600 lines/mm and an Olympus MPlan 100x objective (N.A. = 0.90). Dwell time per sampling spot was two by sixty seconds. The laser power on the sample was of 1.9 mW. A 14 micron long line scan was carried out in the horizontal direction with 30 points on each line. The interval between points was of 0.48 μm. The lateral resolution of the confocal Raman microscope was of ~1 μm.

Cross-Polarization Magic Angle Spinning Carbon 13-Nuclear Magnetic Resonance (CP/MAS ^{13}C-NMR) spectroscopy

The wood, holocellulose and pulp samples were wetted with deionised water (40 to 60% water content) and packed uniformly in a 7 mm zirconium oxide rotor. Recording spectra on wet samples gives a higher apparent resolution than on dry samples.[15] CP/MAS ^{13}C-NMR spectra were recorded using a Bruker 600 MHz™. All measurements were performed at 290 (± 1) K. The Magic Angle Spinning (MAS) rate was of 10 kHz. A double air-bearing probe was applied. Acquisition was performed with a Contact Pulse (CP) sequence using a 4.3 μs proton 90 degree pulse, an 800 μs ramped (100-50%) falling contact pulse and a 2.5 s delay between repetitions. A TPPM15 pulse sequence was used for ^{1}H decoupling. The Hartman-Hahn matching procedure based on glycine was applied. Chemical shift is related, as usual, to tetramethylsilane [TMS ((CH_3)$_4$Si)]. The data point of maximum intensity in glycine carbonyl line was assigned to a chemical shift of 176.03 ppm.

Calculation of cellulose crystallinity (CrI)

In CP/MAS ^{13}C-NMR, the peak deconvolution method was used to integrate the crystalline and non-crystalline peaks in the C4 region for the pulp samples produced from different clones and species. In a typical spectrum, the signal at 86-92 ppm corresponds to the C4 of the highly-ordered cellulose of the crystallite interiors, whereas the broader up-field signal (79-86 ppm) has been assigned to the C4 of non-crystalline cellulose, as well as to the less ordered cellulose chains of the crystallite surfaces.[16,17] Cellulose crystallinity was determined, according to Teeäär,[18] from the area of the crystalline (86-92 ppm) (a) and non-crystalline (79-86 ppm) cellulose C-4 signal (b) as:

$$CrI = \frac{a}{a + b} \tag{1}$$

Atomic force microscopy

Wood, holocellulose and pulp fibres were rapidly frozen in nitrogen slush and freeze-dried to prevent distortion of the cell wall structure caused by air-

drying. The fibres were then embedded in an epoxy resin and transversely sectioned into 1 μm thick sections, using a microtome. These sections were imaged using a Solver P47H™ AFM. Images were taken in height mode, where deflection of the cantilever was used to measure the z position, as well as in phase mode, where the phase lag of the cantilever was used to determine the differences in material stiffness. Image analysis (Image Pro® Plus – Version 6.0) was used to quantify the 'aggregate' zone (area in the secondary layer assumed to be occupied by cellulose) and 'matrix' area in 1 μm by 1 μm scans of

the cell walls of wood and pulp fibres. The 'matrix' area is the zone occupied by lignin-hemicelluloses-extractives in wood, and by lignin-hemicelluloses in pulp. The 'aggregate' area in 1 μm by 1 μm scans of the cell walls of wood, chlorite-delignified wood, acid bisulphite 'raw' pulp and 'D1' pulp is the zone in the secondary layer assumed to be occupied by cellulose (grey area in Fig. 3). The 'matrix' area is assumed to be the area occupied by lignin-hemicelluloses-extractives (red area in Fig. 3) in wood, and by lignin-hemicellulose in the chlorite-delignified wood, acid bisulphite 'raw' pulp and 'D1' pulp.
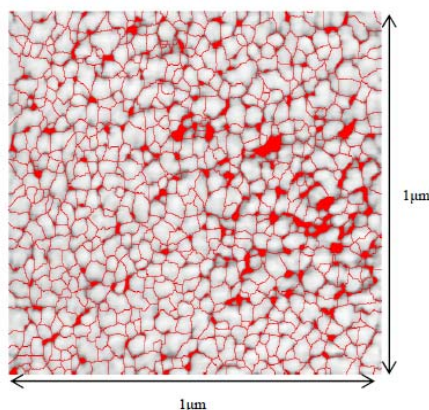

Figure 3: AFM image (1 μm by 1 μm) of the secondary layer within the wood cell wall

The 'aggregate' and 'matrix' areas, determined with 1 μm by 1 μm images, were corrected for wood cell wall thickness. To get the corrected 'aggregate' area for the pulp fibre wall, the relative cell wall thickness needs to be determined (Equation 2):

$$Relative\,cell\,wall\,thickness = \frac{Cell\,wall\,thickness\,of\,pulp\,sample}{Cell\,wall\,thickness\,of\,wood}$$

Equation 3 gives the corrected 'aggregate' area for a particular pulp sample:
Corrected 'aggregate' area = 'aggregate' area of samples x relative cell wall thickness   (3)

Wet chemical properties
Acid-insoluble lignin was determined[19] by gravimetric analysis, according to TAPPI method TM 222. The acid-soluble lignin content was determined by ultraviolet (UV) spectroscopy in accordance with TAPPI method UM 250.[20]

RESULTS AND DISCUSSION
Confocal Raman scans of wood, chlorite-delignified samples, acid bisulphite 'raw' pulp and 'D1' stage pulp
To understand the lignin distribution in the cell wall, the total lignin content in wood, 4 and 9 h holocellulose, acid bisulphite 'raw' pulp and acid

bisulphite-pulped, oxygen-delignified, washed 'D1' pulp were determined by gravimetric analysis and UV spectrometry. Table 1 presents the results of the total lignin content in wood, holocellulose, 'raw' and 'D1' pulp samples. The total lignin contents in *E. gu*, *E. dunnii*, *E. nitens* wood (*i.e.* 29.4, 29.6 and 27.6%, respectively, Table 1) were lower than in the *E. gc* wood (*i.e.* 32.5%, Table 1). The total lignin contents decreased after each delignification process, with the 'D1' pulp samples having the lowest total lignin content throughout. The 4 and 9 h chlorite delignification processes reduced the total lignin content by 40 and 60%, respectively, in contrast to the acid bisulphite pulping and oxygen delignification processes, which resulted in an average lignin reduction of 85 and 92%, respectively, for all wood clones and species investigated. The reason of the significant reduction in lignin content after acid bisulphite pulping was the removal of lignin in the middle lamella, followed by a further ca. 50% lignin reduction during oxygen delignification.

Confocal Raman spectroscopy was used to investigate the distribution of lignin within the cell wall of the wood and chlorite-delignified

(holocellulose) samples. The attempts to analyze acid bisulphite 'raw' and 'D1' stage pulps were unsuccessful, since the total lignin content in the pulp samples was below the lignin detection limit of the confocal Raman instrument, *i.e.* ca. 8%. The Raman lignin intensities in the S and ML regions were used to determine the ratio of Raman intensity in each region.

Equation 4 shows the ratio of Raman intensity in the S regions: Ratio of Raman lignin intensity in S layer = Raman intensity in S layer / Total Raman intensity   (4)

Table 1
Total lignin in wood, 4 and 9 h holocellulose, acid bisulphite 'raw' pulp and 'D1' stage pulp

	Total lignin (%)				
	Wood	4 h holocellulose	9 h holocellulose	'Raw'	'D1'
E. gc	32.5	18.4	10.3	4.3	2.2
E. gu	29.4	20.4	9.6	4.6	2.8
E. dunnii	29.6	18.5	10.0	4.8	2.3
E. nitens	27.6	18.1	11.9	5.3	2.0

Table 2
Confocal Raman intensity in the wood cell walls and distribution of lignin in the S and ML layers

Clones/Species	Raman intensity (Arbitrary units)		Ratio of Raman intensity[*]		Total lignin	
	S layer	ML layer	S/Total lignin	ML/Total lignin	S layer (%)	ML layer (%)
E. gc	491	285	0.63	0.37	20.5	12.0
E. gu	1542	1384	0.52	0.48	15.3	14.1
E. dunnii	428	339	0.56	0.44	16.6	13.0
E. nitens	434	421	0.51	0.49	14.1	13.5

[*]Ratio of Raman intensity in each of the layers relative to Raman Total lignin intensity

A similar formula can be used for determining the Raman intensity ratio in the ML layer. Table 2 shows the Raman lignin intensity, Raman lignin intensity ratios and lignin distribution for both the S and ML regions. The results illustrated in Figure 4 show that, for the *E. gu*, *E. dunnii* and *E. nitens* wood species, 15.3, 16.6 and 14.1%, respectively, of the total lignin is located in the S region of the cell wall, whereas, for the *E. gc* clone, 20.5% of the total lignin is located in the S region (Table 2). The results also show that the *E. gu*, *E. dunnii* and *E. nitens* species have 14.1, 13.0 and 13.5% of the total lignin in the ML region, respectively, whereas, in *E. gc*, 12% of the total lignin is located in the ML region (Table 2).

Subjecting the wood clones and species to a 4 h chlorite delignification resulted in the preferential removal of lignin from the ML region, with some lignin removal from the S region. However, this was not the case for the *E. gc* clone, where lignin was removed from the ML and S regions in equal proportions. The *E. gu* and *E. dunnii* holocellulose showed the lowest amount of lignin. The 4 h chlorite delignification removed 40% of the lignin from the ML and 2%, respectively, from the S region, which contrasted with the *E. nitens* holocellulose, which had the highest amount of lignin, as, in this case, the 4 h chlorite delignification removed 30% of lignin from the ML and 1% from the S region. Figure 4 and Table 1 show a similar trend for the 9 h chlorite delignification, *i.e.* with the exception of the *E. gc* clone, lignin removal occurs preferentially from the ML region, the removal from the S region being limited. For the *E. gc* clone, lignin was removed from the ML and S regions in equal proportions, which suggested that, when lignin is evenly distributed between the S and ML regions, the wood samples are more difficult to delignify. These results demonstrate that confocal Raman spectroscopy is capable of revealing the location and proportion of lignin present in the S and ML regions of the cell walls for *Eucalyptus* wood and chlorite-delignified holocellulose.

CP/MAS ^{13}C-NMR determination of crystallinity in wood, chlorite-delignified wood, acid bisulphite 'raw' pulp and 'D1' pulp

The above results evidence several similarities in the responses of individual clones and species to the changes induced during different delignification processes. Cellulose crystallinity (CrI) in wood and chlorite-delignified holocellulose, determined by CP/MAS ^{13}C-NMR, is shown in Figure 5. In wood, the CrI for the two clones and two species varied between 0.20 and 0.29, the *E. gu* clone having the highest crystallinity (0.29) (Fig. 5). After 4 h chlorite delignification, an increase in crystallinity could be observed, the *E. gc*, *E. gu* and *E. dunnii* showing similarly high levels. A further increase in crystallinity occurred after the 9 h chlorite delignification, the effect being more pronounced in the *E. gc* and *E. dunnii* samples.

Figure 6 illustrates cellulose crystallinity in wood, acid bisulphite 'raw' pulp and 'D1' pulp. After acid bisulphite pulping (Fig. 6), a significant increase in crystallinity was noticed for all clones and species studied. 'Raw' pulp crystallinity varied between 0.35 and 0.39 for the two clones and two species, the *E. nitens* samples showing the highest level (*i.e.*, 0.39). After subsequent oxygen delignification, the *E. gu* clone showed an increase in crystallinity, from 0.36 to 0.41. The *E. gc* clone and the *E. dunnii* and *E. nitens* species showed minimal or no changes after oxygen delignification.
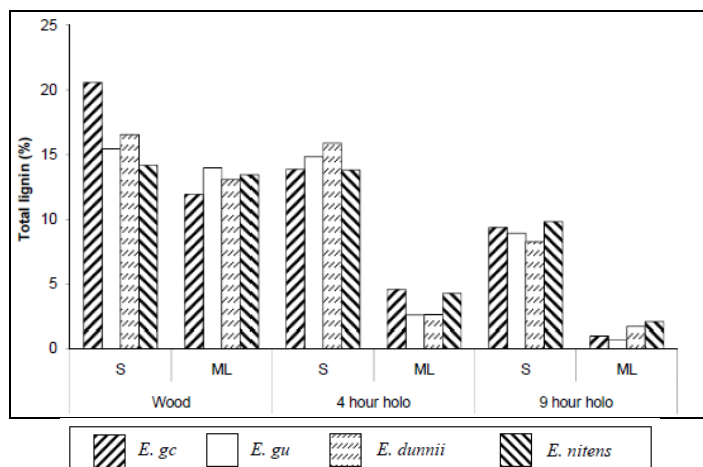

Figure 4: Raman lignin distribution in the secondary and middle lamella layers during delignification
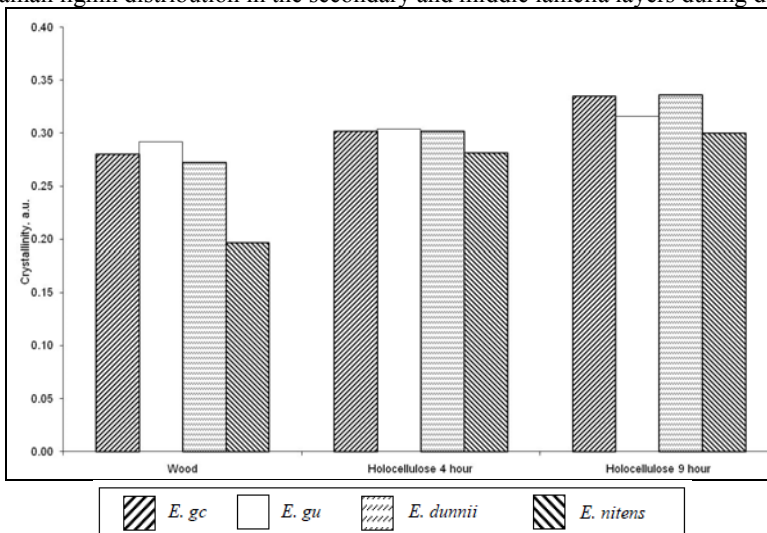

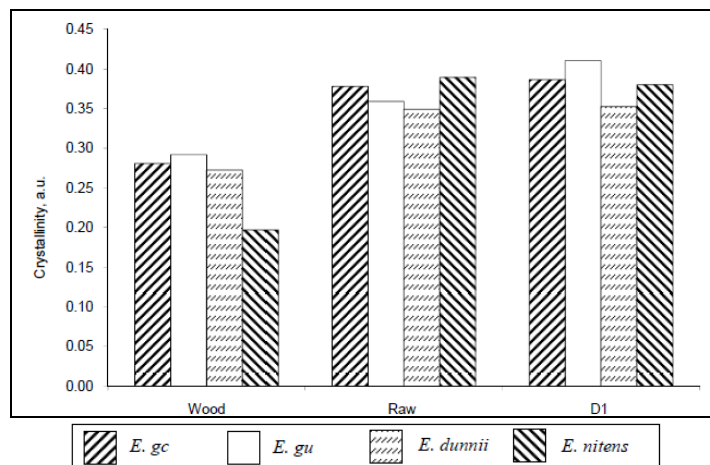Figure 5: Crystalline cellulose determined by solid state NMR in wood and chlorite-delignified holocellulose

Figure 6: Crystalline cellulose determined by solid state NMR in wood, acid bisulphite 'raw' pulp and 'D1' pulp

Table 3
Cellulose 'aggregate' area (μm^2) and 'matrix' area (μm^2) in the 4 and 9 h holocellulose, acid bisulphite 'raw' pulp and 'D1' stage pulp

Clones/ Species		Area (μm^2)				
			Chlorite delignification		Acid bisulphite pulping	
		Wood	4 h holocellulose	9 h holocellulose	'Raw'	'D1'
E. gc	Cellulose 'aggregate' area	1.200	1.050	1.050	1.300	1.300
	'Matrix' area	0.043	0.042	0.021	0.028	0.015
E. gu	Cellulose 'aggregate' area	0.920	1.050	1.050	1.400	1.600
	'Matrix' area	0.057	0.037	0.037	0.040	0.038
E. dunnii	Cellulose 'aggregate' area	1.050	1.050	1.050	1.100	1.200
	'Matrix' area	0.038	0.037	0.016	0.038	0.028
E. nitens	Cellulose 'aggregate' area	0.900	1.050	1.040	1.300	1.500
	'Matrix' area	0.043	0.037	0.026	0.038	0.035

It is evident, from the results shown in Figures 5 and 6, that acid bisulphite pulping caused the highest increase in crystallinity. This is likely to be attributed to the removal of the 'matrix', *i.e.* lignin, hemicelluloses and extractives, during acid bisulphite pulping, resulting in a closer association of cellulose molecules and an increase in the 'aggregate' area.

AFM determination of cellulose 'aggregate' and 'matrix' area in wood, chlorite-delignified wood, acid bisulphite 'raw' pulp and 'D1' pulp

The cellulose 'aggregate' and 'matrix' areas for the different clones and species of wood after chlorite delignification are presented in Table 3. Upon chlorite delignification, an increase in the cellulose 'aggregate' area for the *E. gu* clone and *E. nitens* species was observed, along with a decrease for the *E. gc* clone and *E. dunnii* species. There were marginal differences between the cellulose 'aggregate' areas of the 4 and 9 h

chlorite-delignified samples. Upon acid bisulphite pulping, an increase in cellulose 'aggregate' area occurred for all *Eucalyptus* clones and species (Table 3). The extent of increase varied among the different clones and species. The *E. nitens* species and *E. gu* clone showed the highest increase, the cellulose 'aggregate' area increasing from ca. 0.9 μm^2 (wood) to 1.3 and 1.4 μm^2, respectively. The *E. gc* clone and *E. dunnii* species showed the lowest increase in the cellulose 'aggregate' area (Table 3). A similar trend was observed after subsequent oxygen delignification, the 'D1' stage, for both clones and species.

The 4 h chlorite delignification process reduced the 'matrix' area in the *E. gu* clone from 0.057 to 0.037 μm^2, and in the *E. nitens* species - from 0.043 to 0.037 μm^2 (Table 3). The *E. gc* and *E. dunnii* clone and species showed a marginal decrease in the 'matrix' area after the 4 h chlorite delignification. Further reduction in the 'matrix'

area occurred after the 9 h chlorite delignification with the *E. gc* clone and *E. nitens* species, with a similar response as for the 4 h chlorite delignification. The *E. gc* clone and *E. dunnii* species showed the largest drop in the 'matrix' area after the 9 h chlorite delignification, of around 50%. Acid bisulphite pulping resulted in a reduction of the 'matrix' area for clones and species, with the exception of *E. dunnii*. Further reduction in the 'matrix' area occurred after oxygen delignification with chlorine dioxide washing, *i.e.* the 'D1' stage, the *E. gc* clone showing the greatest decrease, from 0.028 to 0.015 μm^2.

CONCLUSIONS

A series of *Eucalyptus* clones and species were chosen to demonstrate the wide range of lignocellulosic composition. The results obtained evidenced similarities in the response of individual clones and species to the changes induced during chlorite delignification, acid bisulphite pulping and acid bisulphite pulping followed by oxygen delignification. The confocal Raman results for wood and chlorite-delignified holocellulose showed that the middle lamella had low levels of lignin, compared to the secondary cell wall layer, for all clones and species investigated. The *E. gc* clone showed higher levels of lignin in the secondary cell wall layer, compared to the *E. gu* clone, *E. dunnii* and *E. nitens* species. This hardwood clone, *i.e. E. gc*, showed a better response to the delignification processes applied than the other clones and species.

An increase in cellulose crystallinity was observed during chlorite delignification, acid bisulphite pulping and subsequent oxygen delignification. The largest change in crystallinity occurred after acid bisulphite pulping, accompanied by an increased cellulose 'aggregate' area, and a corresponding decrease in the 'matrix' area for each clone and species. This effect could be attributed to the removal of the 'matrix', *i.e.* lignin, hemicelluloses and extractives in wood, during acid bisulphite pulping, resulting in a closer association of cellulose molecules and in an increase of the 'aggregate' area. The present study indicated that confocal Raman spectroscopy, CP/MAS ^{13}C-NMR and Atomic Force Microscopy are useful in investigating the lignocellulosic composition of wood, chlorite-delignified holocellulose, acid bisulphite pulp and acid bisulphite oxygen-delignified washed pulp.

REFERENCES
[1] M. Foston and A. J. Ragauskas, *Biomass Bioenerg.*, **34**, 1885 (2010).
[2] U. P. Agarwal, *Planta*, **224**, 1141 (2006).
[3] W. A. Côte, Jr., "Wood Ultrastructure – an Atlas of Electron Micrographs", University of Washington Press, Syracuse, NY, USA, 1967.
[4] W. N. Haworth, *Helv. Chim. Acta*, **11**, 534 (1928).
[5] E. Sjöström, "Wood Chemistry – Fundamentals and Applications" 2nd ed., Academic Press, San Diego, USA, 1993.
[6] K. Schenzel, S. Fischer and E. Brendler, *Cellulose*, **12**, 223 (2005).
[7] U. P. Agarwal, R. S. Reiner and S. A. Ralph, *Cellulose*, **17**, 721 (2010).
[8] L. Segal, J. J. Creely, A. E. Martin and C. M. Conrad, *Text. Res. J.*, **29**, 786 (1959).
[9] G. Jayme and H. Knolle, *Papier*, **18**, 249 (1964).
[10] K. Leppänen, S. Andersson, M. Torkkeli, M. Knaapila, N. Kotelnikova and R. Serimaa, *Cellulose*, **16**, 999 (2009).
[11] F. Horii, A. Hirai and R. Kitamaru, *Macromolecules*, **20**, 2117 (1987).
[12] R. H. Newman and J. A. Hemmingson, *Holzforschung*, **44**, 351 (1990).
[13] R. H. Newman, *Solid State Nucl. Mag. Res.*, **15**, 21 (1999).
[14] S. H. D. Hulleman, J. M. Van Hazendonk and J. E. G. Van Dam, *Carbohydr. Res.*, **261**, 163 (1994).
[15] R. H. Newman, J. A. Hemmingson and I. D. Suckling, *Holzforschung*, **47**, 234 (1993).
[16] D. L. VanderHart and R. H. Atalla, *Macromolecules*, **17**, 1465 (1984).
[17] K. Wickholm, P. T. Larsson and T. Iversen, *Carbohydr. Res.*, **312**, 123 (1998).
[18] R. Teeäär, R. Serimaa and T. Paakkari, *Polym. Bull.*, **17**, 231 (1987).
[19] TAPPI method TM 222 om-83, in "Test Methods 1998-1999", TAPPI Press, Atlanta, USA, 1999.
[20] TAPPI useful method UM 250 um-83, in "Test Methods 1998-1999", TAPPI Press, Atlanta, USA, 1999.